Macromolecules
ARTICLE

Macromolecules **2009**, *42*, 7545–7552 **7545**
DOI: 10.1021/ma9008912

Isothermal Titration Calorimetry: A Powerful Technique To Quantify Interactions in Polymer Hybrid Systems

Khalid Chiad, Simon H. Stelzig, Radu Gropeanu, Tanja Weil, Markus Klapper,* and Klaus Müllen*

Max-Planck-Institute for Polymer Research, Ackermannweg 10, 55128 Mainz, Germany

Received April 23, 2009; Revised Manuscript Received July 17, 2009

ABSTRACT: Isothermal titration calorimetry (ITC) was introduced as a highly sensitive tool to analyze interactions in polymer and material science by their thermodynamic patterns. The thermodynamic parameters ΔH, ΔS, ΔG, K_B, and the stoichiometric ratio of the interactions in a complex organic−inorganic hybrid system were determined in a single experiment. In particular, the adsorption behavior of surface-active amphiphilic copolymers, bearing different types of anchor groups (nonionic, zwitterionic, and acidic), with SiO_2 nanoparticles in a multicomponent solvent system was investigated. The knowledge of the thermodynamic parameters of the interaction provided, beside its strength, a detailed understanding of its mechanism. Particularly, for the production of the nanocomposites, this knowledge might lead to a more rational and optimized design of these materials.

Introduction

Isothermal titration calorimetry (ITC) has recently evolved from an expert technology to a major, commercially available tool, allowing the analysis and interpretation of molecular interactions in biological systems.[1] This method is based on the repetitive addition of a solution of one of the interacting molecules (ligand, L), via automated injection at constant temperature, into a cell containing a solution of the second molecule (macromolecule, M). By measuring the release (exothermic reaction) or the absorption (endothermic reaction) of heat due to the formation of a complex (ML), the interaction between the components is quantified.[2] ITC has gained much attention for studying different kinds of binding events in biochemical processes on the basis of their thermodynamic parameters. Host−guest interaction of protein−protein,[3] small molecule/drug−protein,[4] DNA−drug interactions,[5] and enzyme kinetics or antibody activity have already been successfully examined by ITC.[6]

To investigate the intermolecular interactions and their binding equilibria, ITC competes with several already established methods, for instance fluorescence, UV/vis[7] and NMR[8,9] spectroscopy, surface plasmon resonance (SPR),[10] and analytical ultracentrifugation (AUC)[11] (Table 1). However, all these techniques have certain drawbacks, such as the requirement of large quantities of the samples, the necessity to introduce labels, or long measurement times. In contrast, ITC offers a fast calorimetric response and thermal equilibration combined with a simple sample preparation.[12] The most important features of ITC include the determination of the entire thermodynamic profile (ΔH, ΔS, ΔG, K_B, and the stoichiometry n) of an interaction in only one experiment. Since ITC is less common in polymer and material science,[13] a comparison of the strengths and weaknesses of comparable methods, as given in Table 1, seems appropriate.

In polymer and material science, interactions between various components play a decisive role, as for example in the formation of organic−inorganic hybrid systems, adsorbates,[17] and micelles.[18] Therefore, the use of ITC is herein extended from its original utilization in biological system into this direction. To demonstrate the applicability of ITC in materials sciences, the surface modification of inorganic particles as this is a key step in the production of organic−inorganic hybrid systems have been chosen. This process is mainly based on a noncovalent adsorption of amphiphilic compounds (e.g., surfactants, amphiphilic copolymers) on the surface of an inorganic material.[19] A very important parameter thereby is the strength and irreversibility of the adsorption of the surface active compound on the inorganic material. For example, processing of these hybrid materials by extrusion (a major technique to manipulate hybrid materials) exerts a tremendous external shear force, which might cause the surface active compound to desorb from the inorganic material.[20] Such a behavior destabilizes the particles in the polymeric matrix and results in aggregates. While investigations of this adsorption process have already been performed by using common batch or flow reaction calorimeters, but yielding only ΔH by a complex data evaluation,[21−26] ITC is capable to determine several other important thermodynamic parameters (ΔH, ΔS, K_B, ΔG, stoichiometric ratio) by a single experiment. These values provide quantification and detailed understanding of the adsorption process of surface-active molecules onto inorganic particles. In this way, a direct correlation between the adsorption strength and structure of the surface active compounds could be achieved. Above all, knowledge of the adsorption mechanism in combination with the structure provided by ITC should facilitate a more rational design into the mainly empirically based production and optimization of nanocomposites.

This versatility of ITC is demonstrated by investigating the interaction of SiO_2 nanoparticles with surface-active amphiphilic copolymers consisting of 2-ethylhexyl methacrylate (EHMA) as the hydrophobic part and poly(ethylene oxide) methacrylate (PEOMA), 4-vinyl-1-(3-sulforopyl)pyridinium inner salt (4VPSB), and (ethylene glycol) methacrylate phosphate (EGMP) in a multicomponent solvent system (Figure 1).[27] Hereby, PEOMA was chosen as a representative of the class of nonionic anchor groups, 4VPSB as zwitterionic anchor group,

*Corresponding authors. E-mail: klapper@mpip-mainz.mpg.de (M.K.), muellen@mpip-mainz.mpg.de (K.M.).

Published on Web 09/02/2009

Table 1. Standard Techniques for the Determination of Binding Constants

method	signal	information	advantage	disadvantage
spectroscopy (fluorescence, UV/vis, CD)	change of absorption or emission of light	K_B (10^4−10^{11} M^{-1})	in solution	probe needed, intervention due to labeling[7]
nuclear magnetic resonance	shift of magnetic resonance frequency	K_B (10^3−10^6 M^{-1})	in solution, structural information	slow, large sample, expensive[8]
surface plasmon resonance (SPR)	change of relative index due to mass	K_B (10^3−10^{13} M^{-1}), k_{+1}, k_{-1}	small sample, automated	surface coupled, high molecular mass of the ligand required, expensive[10]
analytical ultracentrifugation (AUC)	absorption at different radii for different times	K_B (10^3−10^8 M^{-1})	good for homomeric interactions	slow, particle density
stopped-flow	coupled to spectroscopy	K_B (10^3−10^{12} M^{-1}), k_{+1}, k_{-1}	fast	probe needed[14]
radioligand binding assay	various, e.g., SDS-PAGE, radio activity densitometry	K_B (10^3−10^{15} M^{-1})	mix-and-read, labeling step does not change affinity, high-throughput	radioactivity, receptor immobilization[15,16]
microcalorimetry (ITC)	heat of binding	K_B (10^3−10^{11} M^{-1}), ΔH, ΔS, ΔC_p, n	in solution, no labels, automated, direct access to ΔH, ΔS, K_B	large sample size

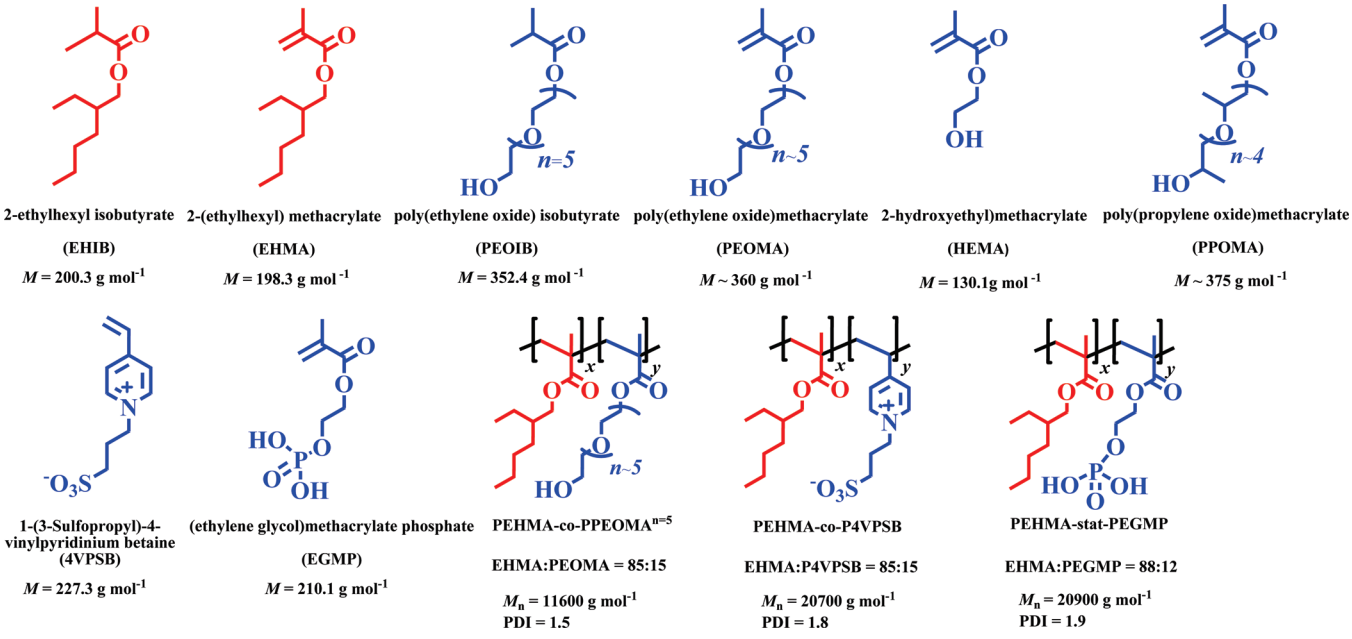

Figure 1. Chemical structure and molar mass of the monomers and amphiphilic copolymers used in this study.

and EGMP as an acidic anchor group. SiO_2 was selected as the inorganic material due to its enormous relevance in the area of nanocomposites as impact modifiers and as additive to improve scratch resistance.[28]

Experimental Section

Materials and Methods. 2-Ethylhexyl methacrylate (EHMA), poly(ethylene oxide) methacrylate (PEOMA$^{n\approx5,9}$), 4-vinylpyridine (4VP), (ethylene glycol) methacrylate phosphate (EGMP), 1,3-propane sultone, 2-ethyl-1-hexanol, isobutyryl chloride, and hexaethylene glycol were purchased from Aldrich and used as received. Methacryloyl chloride was obtained from Fluka. SiO_2 nanoparticles, with an average diameter of ~10 nm, were donated as a 30 wt % aqueous dispersion from Merck KGaA. 2-Ethylhexyl isobutyrate (EHIB) and poly(ethylene oxide) isobutyrate (PEOIB) were prepared from methacryloyl chloride and 2-ethyl-1-hexanol and hexaethylene glycol, respectively. Therefore, 2-ethyl-1-hexanol/hexaethylene glycol (25 mmol) was dissolved in 80 mL of dichloromethane and triethylamine (25 mmol) was added. The mixture was cooled to 0 °C, and isobutyryl chloride (26 mmol), dissolved in 20 mL of dichloromethane, was slowly added over a period of 30 min. After stirring for 24 h, the formed white precipitate was filtered off. The resulting solution was washed twice with 25 mL of brine and twice with 10 wt % aqueous solution of sodium hydrogen carbonate. After drying the extract with anhydrous sodium sulfate, colorless oil remained (75% yield). 1-(3-Sulfopropyl)-4-vinylpyridinium betaine (4VPSB) was prepared according to the described procedure in the literature.[29] The amphiphilic copolymers PEHMA-*co*-PPEOMA$^{n\approx5}$, PEHMA-*co*-PEGMP, and PEHMA-*co*-P4VPSB were prepared by free radical polymerization of EHMA and PEOMA$^{n\approx5}$, EGMP, and 4VPSB, respectively, as described in the literature (molar ratio of EHMA:PEOMA$^{n\approx5}$ = 85:15, EHMA:PEGMP = 88:12, and EHMA: P4VPSB = 85:15).[30]

Description of the ITC Titration Experiment. *Sample Preparation.* The ITC instrument used was a VP-ITC microcalorimeter (Microcal, Inc., Northampton, MA), which operated at constant temperature of 298 K. To carry out a binding experiment, the inorganic nanoparticle solution (55.6 μL of an aqueous SiO_2 dispersion (30 wt % in H_2O) in 1.5 mL of 1,4-dioxane, 0.5 mL of ethanol) was placed in the sample cell and the reference cell filled with the solvent mixture (1.5 mL of 1,4-dioxane, 0.5 mL of ethanol, and 46.8 μL of H_2O). Both cells were mounted in an adiabatic chamber, whose temperature was

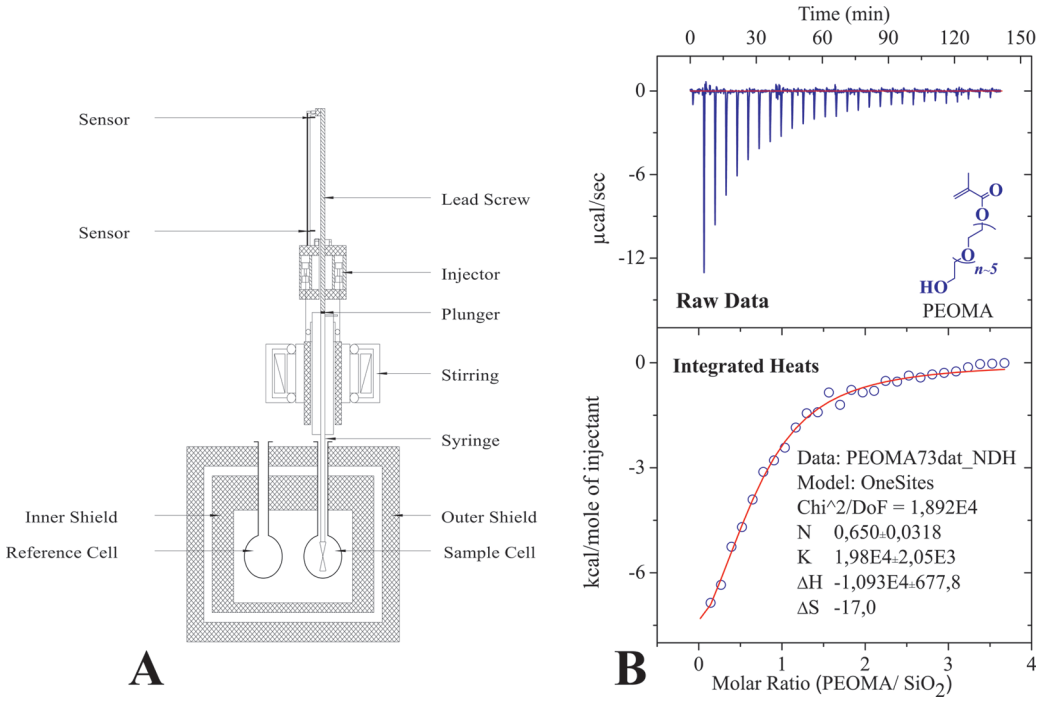

Figure 2. (A) Schematic illustration of the ITC instrument, showing the two cells (sample and reference) surrounded by the thermostatic jacket, the injection syringe that also acts as stirring device. (B) Experimental curve for the titration of a 278 mM solution of poly(ethylene oxide) methacrylate (PEOMA$^{n\approx5}$) in 1,4-dioxane/ethanol/H_2O into a dispersion of SiO_2 (10 mg mL^{-1}) in the same solvent at 298 K; the upper panel shows the thermal power (dQ/dt) obtained during the injection. The lower panel illustrates the titration curve, which is obtained by the integration of the peaks from the upper panel, together with a line of best fit, to estimate ΔH, ΔG, K, and the stoichiometry n.

kept constant during the measurement. A long-needle syringe (nominal volume 250 μL), with a twisted paddle fastened to its end, was filled with the solution of the organic compound (EHIB, PEOIB, EHMA, PEOMA$^{n\approx5}$, PEOMA$^{n\approx9}$, HEMA, PPOMA$^{n\approx5}$, 4VPSB, EGMP, and the copolymers PEHMA-*co*-PPEOMA$^{n\approx5}$, PEHMA-*co*-P4VPSB, and PEHMA-*co*-PEGMP) in 7.5 mL of 1,4-dioxane, 2.5 mL of ethanol, and 233.8 μL of H_2O. The syringe was placed inside the sample cell, and the entire syringe assembly was rotated continuously to provide proper mixing of the content of the sample cell within a few seconds after an injection (Figure 2A).[31]

ITC Measurement. After reaching the thermal equilibrium, the injection of the ligand (copolymer) was automatically conducted stepwise until the surface of the SiO_2 was saturated with the ligand. The first injection was set to very small volume of 1.5 μL (due to the possible dilution during the equilibration time preceding the measurement and then the first injection was ignored in the analysis of data)[32] and was followed by 27 injections of 10 μL each. The chosen time interval between two consecutive injections was 300 s in order to ensure that the thermodynamic equilibrium was reached prior to the next injection. To illustrate the ITC experiment, a characteristic output of an ITC thermogram was depicted in Figure 2B, showing the titration of a 278 mM solution of poly(ethylene oxide) methacrylate (PEOMA$^{n\approx5}$) in 1,4-dioxane/ethanol/H_2O into a dispersion of SiO_2 (10 mg mL^{-1}) in the same solvent at 298 K. The upper section of Figure 2B represents the raw data as supplied by the instrument and the progression of the experiment in time. The peaks corresponded to the individual aliquots of added macromolecule solution, and the current applied for the compensation of the reaction heat was plotted in energy units against time. The lower part of Figure 2B showed the titration curve, resulting from the integration of the individual peaks and plotted as ΔH in kcal/mol against the molar ratio macromolecule/SiO_2.

Dilution Experiment. In order to subtract the influence of the enthalpy of dissolving the ligand, a dilution experiment was conducted. In this experiment the ligand was injected into the sample cell, containing only the solvent mixture. The released/absorbed heat caused by the solvent enthalpy was subtracted from the data obtained from the titration of the SiO_2 nanoparticles with the monomers or copolymers (Figure 3). After this subtraction, the normalized heat was plotted against the molar ratio of the polymer versus the inorganic particle.

Data Analysis. The data analysis was performed using the ORIGIN 7.0 based software. The thermodynamic parameters (K_B, ΔH) were estimated as adjustable parameters in the fitting procedure: one set of sites and two set of sites, to the experimental data using a nonlinear least-squares approach (Levenberg−Marquardt algorithm).[33,34] For a ligand L binding to a single set of n identical sites on a host molecule M, i.e.

$$M + L = ML$$

$$ML + L = ML_2$$

$$ML_{n-1} + L = ML_n$$

where the single-site binding constant was[12,34]

$$K_B = \frac{[ML]}{[M][L]} \quad (1)$$

The total concentration of the macromolecule [M_T] was the sum of concentration of the free macromolecule [M] plus the one of the formed complex [ML], and the total concentration of the ligand [L_T] was the sum of the free ligand [L] plus the one of the formed complex [ML]:

$$[M_T] = [M] + [ML] \quad (2)$$

$$[L_T] = [L] + [ML] \quad (3)$$

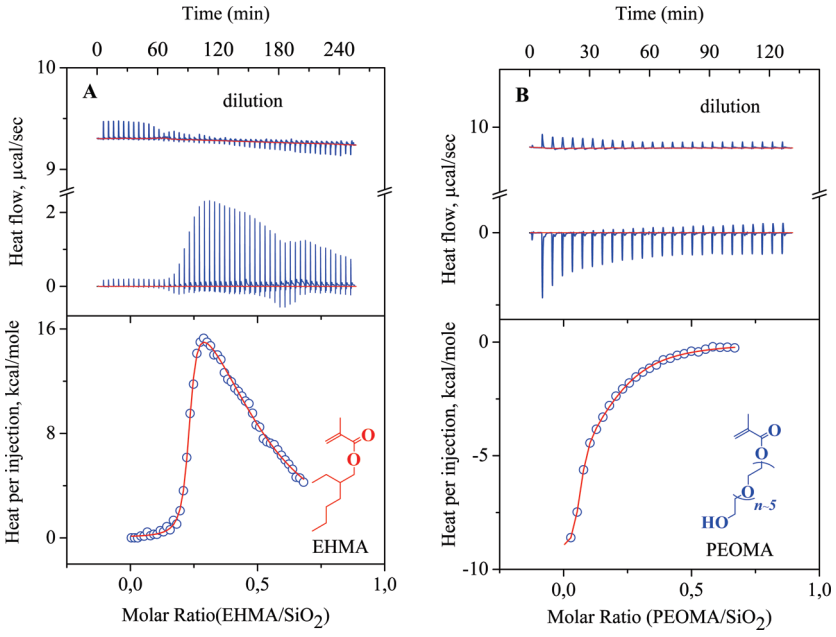

Figure 3. Binding isotherms for the titration of 55 mM solution of (A) EHMA and (B) PEOMA$^{n\approx5}$ in 1,4-dioxane/ethanol/H_2O into a dispersion of SiO_2 (10 mg mL^{-1}) in the same solvent at 298 K.

From these relations resulted that

$$[M] = [M_T] - [ML] \quad \text{and} \quad [L] = [L_T] - [ML] \tag{4}$$

From eqs 3, 4, and 1, K_B was evaluated to

$$K_B = \frac{[ML]}{([L_T] - [ML])([M_T] - [ML])} \tag{5}$$

and

$$\Delta G = RT \ln K_B = \Delta H - T\Delta S \tag{6}$$

where ΔG, ΔH, and ΔS were the free energy, enthalpy, and entropy change for single site binding. In addition to the direct measurement of ΔH and the calculation of K_B, the inflection point of the binding isotherm (Figure 2B) allowed for the determination of the stoichiometry of the complex n (the ratio of the copolymer to the inorganic nanoparticle in the complex ML_n, at equilibrium).

Results and Discussion

The interactions of SiO_2 nanoparticles with the hydrophobic monomer EHMA, the hydrophilic monomers PEOMA (with 5 and 9 ethylene oxide units, PEOMA$^{n\approx5}$/PEOMA$^{n\approx9}$), 2-hydroxyethyl methacrylate (HEMA), poly(propylene oxide)methacrylate (PPOMA$^{n\approx5}$), 4VPSB as well as EGMP, and the copolymers PEHMA-*co*-PPEOMA$^{n\approx5}$, PEHMA-*co*-P4VPSB, and PEHMA-*co*-PEGMP were investigated (Figure 1, Table 1). To render such systems applicable for the ITC measurements, appropriate solvent mixtures, which dissolve the surface-active copolymers and disperse the SiO_2 nanoparticles, had to be identified. These solvent mixtures were important to exclude all heat of solvent mixing during the injections, which would influence the measurements in an uncontrolled manner.[2,6] A mixture of 1,4-dioxane, ethanol, and water was chosen, since this solvent mixture guaranteed good solubility of the amphiphilic copolymers and suppressed the formation of aggregates of the inorganic particles during the measurements (the stability of the dispersion of the SiO_2 nanoparticles in the chosen solvent mixture had been investigated by dynamic light scattering). The surface-active compounds (EHMA, PEOMA$^{n\approx5,9}$, HEMA, PPOMA$^{n\approx5}$, 4VPSB, EGMP, PEHMA-*co*-PPEOMA$^{n\approx5}$, PEHMA-*co*-P4VPSB, and PEHMA-*co*-PEGMP) were slowly injected into the silica dispersion, and the resulting heat of interaction was determined. In the first step, the interactions of the inorganic particles with the monomers EHMA, PEOMA$^{n\approx5,9}$, HEMA, and PPOMA$^{n\approx5}$ were analyzed, in order to obtain a better understanding of their role and influence during the interaction. In the second step, the adsorption of the amphiphilic copolymer PEHMA-*co*-PPEOMA$^{n\approx5}$ on the surface of the SiO_2 particles was explored. Moreover, the copolymers PEHMA-*co*-P4VPSB and PEHMA-*co*-PEGMP as well as their corresponding hydrophilic parts 4VPSB and EGMP were applied in an analogous manner to detect the impact of different classes of anchor groups (nonionic versus zwitterionic or acidic) on their adsorption behavior (Table 1). To ensure reproducibility and to increase the accuracy of the results, every experiment was repeated at least three times under the same conditions. To illustrate the potential of the ITC as a novel tool to examine organic−inorganic hybrid materials, the measurements of the ITC experiments for EHMA, PEOMA$^{n\approx5}$, and PEHMA-*co*-PPEOMA$^{n\approx5}$ will be discussed in greater detail. As all other experiments were performed in a similar way only the decisive values will be given.

Interaction of the Low Molecular Weight Model Compounds with SiO_2. *Interaction of EHMA with the SiO_2 Nanoparticles.* In a first series of experiments, EHMA was applied as a model compound to monitor the influence of the hydrophobic part of the copolymers on the adsorption process. Figure 3A shows the ITC curve for the titration of 55 mM solution of EHMA in 1,4-dioxane/ethanol/H_2O into a dispersion of SiO_2 (10 mg mL^{-1}) in the same solvent at 298 K. The observed peaks suggested an endothermic process by each injection. Evaluation of this data by integration followed a nonlinear least-squares approach (Levenberg−Marquardt algorithm)[33,34] which leads to an entropically driven interaction with both positive entropy and positive enthalpy (Table 2). Such a thermodynamic profile, positive ΔH and ΔS, is usually characteristic for hydrophobic interactions.[35−37] In general, ΔH primarily reflects the strength of the noncovalent interactions between

Table 2. Thermodynamic Parameters Obtained by the ITC Measurements of the Studied Surface-Active Compounds with SiO_2 Nanoparticles in a Mixture of 1,4-Dioxane, Ethanol, and H_2O at 298 K

surface-active compound	K_B (mol L^{-1})	ΔH (kcal mol^{-1})	$T\Delta S$ (kcal mol^{-1})	ΔG (kcal mol^{-1})
EHIB[a]	$1.10 \times 10^7 \pm 4.30 \times 10^6$	0.25 ± 0.18	10.19	−9.94
	$1.00 \times 10^5 \pm 1.50 \times 10^4$	63.46 ± 2.70	70.36	−6.88
PEOIB[a]	$3.87 \times 10^4 \pm 1.33 \times 10^4$	-13.60 ± 9.99	−7.33	−6.25
EHMA[a]	$1.90 \times 10^7 \pm 3.00 \times 10^6$	0.04 ± 0.01	9.98	−9.94
	$5.70 \times 10^4 \pm 6.20 \times 10^3$	25.50 ± 1.43	31.90	−6.40
PEOMA$^{n\approx5}$[a]	$6.10 \times 10^4 \pm 6.50 \times 10^3$	-25.13 ± 4.23	−18.60	−6.53
HEMA[b]	$8.26 \times 10^4 \pm 2.27 \times 10^4$	-0.19 ± 0.04	6.49	−8.20
PEOMA$^{n\approx5}$[b]	$6.35 \times 10^3 \pm 0.04 \times 10^3$	-43.50 ± 0.20	−38.16	−5.34
PEOMA$^{n\approx9}$[b]	$1.15 \times 10^5 \pm 2.03 \times 10^4$	-69.87 ± 0.54	−62.90	−6.97
PPOMA$^{n\approx5}$[b]	$1.58 \times 10^5 \pm 0.92 \times 10^4$	-0.05 ± 0.007	7.04	−6.98
4VPSB[a]	$1.74 \times 10^5 \pm 3.05 \times 10^4$	-27.57 ± 2.24	−20.42	−7.14
EGMP[a]	$4.33 \times 10^4 \pm 2.35 \times 10^3$	-39.85 ± 0.8	−33.39	−6.46
PEHMA-*co*-PPEOMA$^{n\approx5}$	$2.50 \times 10^5 \pm 4.40 \times 10^4$	-10.01 ± 0.53	−2.77	−7.33
PEHMA-*co*-P4VPSB	$5.70 \times 10^5 \pm 3.29 \times 10^5$	-8.77 ± 0.20	−0.92	−7.86
PEHMA-*co*-PEGMP	$4.78 \times 10^5 \pm 0.00$	-10.26 ± 0.16	−2.51	−7.75

[a] Concentration of the hydrophilic monomer = 55 mM. [b] Concentration of the hydrophilic monomer = 278 mM.

the monomers/copolymer and the surface of the SiO_2 nanoparticles (e.g., van der Waals, hydrogen bonds, etc.) relative to those existing within the solvent.[38,39] As a result of the obtained values of ΔH for the titration of SiO_2 with EHMA, no interaction of EHMA with the particle surface occurred. The positive value of ΔS could be attributed to a collapse of the so-called "iceberg structure",[40] which was caused by water molecules surrounding the hydrophobic chain of EHMA forming rigid, ice-like assemblies, resembling icebergs. At the same time solvent molecules were transferred from the solvation shell of EHMA to the bulk, which also represented an entropy increasing process.[41,42] The ITC curve in Figure 3A clearly indicates a complex adsorption behavior, since the fitting of these curves revealed that two hydrophobic processes occurred during the titration.

Interaction of PEOMA, HEMA, and PPOMA with the SiO_2 Nanoparticles. The monomers PEOMA, HEMA, and PPOMA were investigated in a similar manner to EHMA. In detail, the binding isotherm of the interaction of a 55 mM solution of PEOMA$^{n\approx5}$ in 1,4-dioxane/ethanol/H_2O into a dispersion of SiO_2 (10 mg mL^{-1}) in the same solvent at 298 K is presented in Figure 3B. A clear exothermic effect for each titration step was observed. This behavior was attributed to a direct interaction between the PEO chain and the hydroxyl groups on the SiO_2 surface.[26,43,44] In this case, the binding enthalpy was found to be negative (−25.13 kcal mol^{-1}) and compensated by a very negative ΔS value (−18.60 kcal mol^{-1}, Figure 5 and Table 2). The obtained binding constant K_B (6.1×10^4 M^{-1}) corresponded to a moderate interaction affinity of this monomer with the surface of the SiO_2 nanoparticles. The dominant negative enthalpy suggested the presence of a large number of van der Waals interactions or hydrogen bonds between the monomer PEOMA and the SiO_2 particles.[43,45] ΔS mainly reflected two contributions concerning the order of the system: changes in solvation entropy and changes in conformational entropy. The change in the solvation entropy occurred during the adsorption process, when the oxygen atom of the EO groups released the associated solvent molecules before interacting with the nanoparticle surface. This process yielded a positive change in entropy. At the same time, the adsorption of PEOMA onto the SiO_2 nanoparticles resulted in the loss of the translational and conformational freedom, which caused a negative change in conformational entropy.[46,47] Since the overall entropy detected by ITC was negative, the highest impact on this term was represented by the change in the conformational freedom.

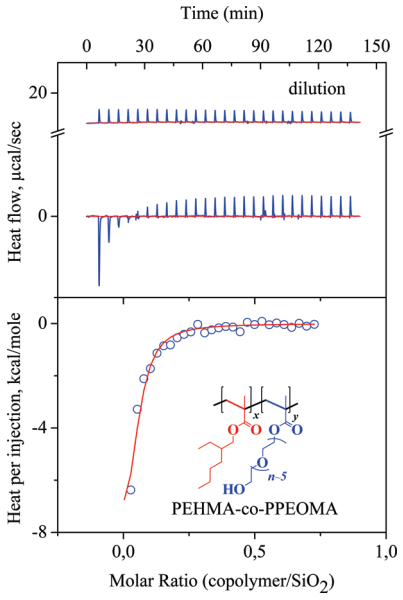

Figure 4. Binding isotherms for the titration of a 55 mM solution of PEHMA-*co*-PPEOMA$^{n\approx5}$ in 1,4-dioxane/ethanol/H_2O into a dispersion of SiO_2 (10 mg mL^{-1}) in the same solvent at 298 K.

Comparing the thermodynamic parameters for the interaction of HEMA, PEOMA$^{n\approx5}$, and PEOMA$^{n\approx9}$, the results indicated that in case of HEMA almost no interaction (ΔH = −0.19 kcal mol^{-1}) with the SiO_2 surface was detected, whereas the strength of the interaction increased with the number of EO units, from PEOMA$^{n\approx5}$ (ΔH = −43.50 kcal mol^{-1}) to PEOMA$^{n\approx9}$ (ΔH = −69.87 kcal mol^{-1}). This was due to the increasing number of hydrogen bonds. The increase showed a concave behavior, which implied a decreasing interaction per EO unit, suggesting an upper limit for the number of interacting EO units.

Accessibility of Surface Groups. In addition, if the EO units were sterically shielded, as in PPOMA$^{n\approx5}$ by a CH_3 group, the interaction dramatically decreased (ΔH = −0.05 kcal mol^{-1}). These results clearly demonstrated that besides a certain number of interacting groups the accessibility of these groups was of great importance for the interaction with the particle surface.

Investigation of Monomers versus Polymers. Because of the fact that all measurements were conducted with monomers, yet the corresponding polymers consisted of their saturated analogues, the influence of the double bond had to be

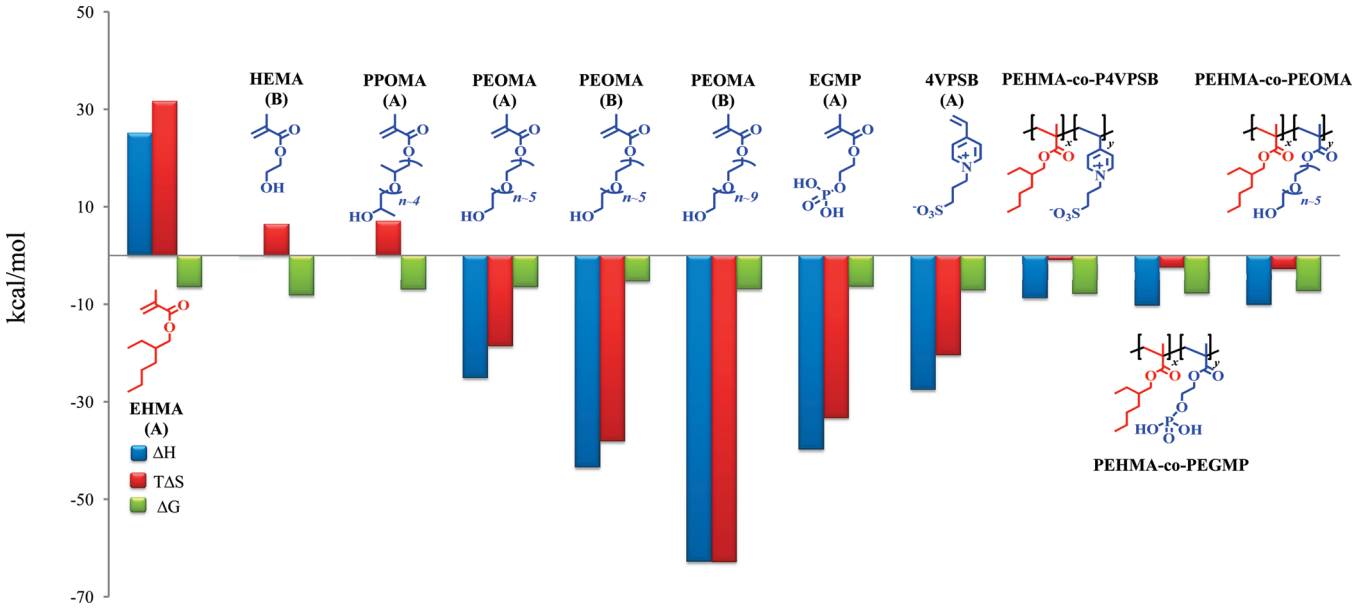

Figure 5. Schematic diagram presenting the thermodynamic profiles observed for all applied compounds: (A) concentration of the hydrophilic monomer = 55 mM; (B) concentration of the hydrophilic monomer = 278 mM.

determined. Hence, the corresponding saturated compounds EHIB (as the analogue of EHMA) and PEOIB (as the analogue of PEOMA) were applied in the ITC measurements. These results displayed an almost identical behavior compared to EHMA and PEOMA, and so, no influence of the double bond on the adsorption behavior was monitored (Table 2). Thus, the hydrophilic monomers can be directly applied in ITC measurements without the need to synthesize either model compounds or the amphiphilic copolymers.

Interaction of the Amphiphilic Copolymers PEHMA-*co*-PPEOMA$^{n\approx5}$, PEHMA-*co*-P4VPSB, and PEHMA-*co*-PEGMP with the SiO_2 Nanoparticles. All the copolymers PEHMA-*co*-PPEOMA$^{n\approx5}$ (M_n = 11 600 g mol^{-1}, PDI = 1.5), PEHMA-*co*-P4VPSB (M_n = 20 700 g mol^{-1}, PDI = 1.8), and PEHMA-*co*-PEGMP (M_n = 20 900 g mol^{-1}, PDI = 1.9) which were proposed as stabilizers of SiO_2 were studied in a similar way as it was described for the low molecular weight compounds. Exemplarily, the results of the titration of SiO_2 particles with the copolymer PEHMA-*co*-PPEOMA$^{n\approx5}$ are presented in Figure 5 (Table 2). The raw data obtained from this experiment resembled the one of PEOMA$^{n\approx5}$. The thermodynamic data exhibited both negative enthalpy and entropy values, supporting this first impression (Figure 5). On the basis of a higher binding constant K_B (2.59×10^5 M^{-1}), a stronger interaction was detected between the copolymer molecules and the surface of the SiO_2 nanoparticles compared to PEOMA$^{n\approx5}$. The measured enthalpy reflected the changes of noncovalent bond energies during the interaction (i.e., hydrogen bond formation), which was dominated by hydrophilic forces. Even though the copolymer consisted of 85 mol % EHMA, which showed a strong endothermic adsorption, the adsorption of the copolymer was exothermic. This behavior is the result of the several binding sites (PEOMA, 4VPSB, and EGMP groups) present in the copolymer. Similar to multidentate ligands, these several anchor groups lead to a strong adsorption on the surface of the particles, contrary to an estimated adsorption strength obtained by adding up the binding enthalpies of the corresponding monomers according to their molar ratios. The adsorption of the monomers PEOMA, 4VPSB, and EGMP were accompanied by a tremendous negative entropy, rendering this adsorption entropically unfavorable, whereas in case of the copolymers this is nearly fully compensated. As a result, the high molecular weight compounds bear a high entropic advantage over the low molecular weight compounds.

The copolymers PEHMA-*co*-P4VPSB and PEHMA-*co*-PEGMP were applied to analyze the difference in the adsorption behavior between a zwitterionic anchor group, an acidic anchor group, and a nonionic anchor group (PEHMA-*co*-PPEOMA$^{n\approx5}$). The adsorption behavior of the corresponding hydrophilic monomers EGMP and 4VPSB revealed a similar behavior to that of PEOMA, i.e., highly enthalpically favorable and highly entropically unfavorable (Table 1, Figure 5). The results identified no significant difference between the zwitterionic anchor group, the acidic anchor group, and the nonionic anchor group. However, this statement is only correct, if in the case of the nonionic anchoring (PEHMA-*co*-PPEOMA$^{n\approx5}$) a sufficient quantity of bonding sites was present, i.e., an adequate number of EO units (number of EO = 5). If this is not the case, as demonstrated for HEMA (number of EO = 0), the nonionic interactions were drastically weaker than the zwitterionic or acidic interactions.

A comparison of all binding experiments performed herein pointed to the existence of different mechanisms for the adsorption processes of the applied compounds. For example, the adsorption of the copolymer PEHMA-*co*-PPEOMA$^{n\approx5}$ and the hydrophilic segment PEOMA revealed an exothermic interaction (i.e., enthalpy-driven process), while in the case of EHMA an endothermic process was found (i.e., entropy-driven process). This outcome suggested different interaction patterns of the monomers as well as the copolymer with the surface of the SiO_2 particles. On the basis of the obtained results for PEHMA-*co*-PPEOMA$^{n\approx5}$, the copolymer showed a similar adsorption behavior as the hydrophilic monomer PEOMA$^{n\approx5}$ (Figure 5). This behavior demonstrated that the hydrophilic side chains of the copolymer adsorbed on the surface of the particles, whereas the hydrophobic side chains, bearing no interaction with the particle surface, protruded into the solution (Figure 6).

The results for the amphiphilic copolymer PEHMA-*co*-PPEOMA demonstrated that its adsorption behavior is mainly determined by its hydrophilic component and that the double bond of the corresponding monomers had no

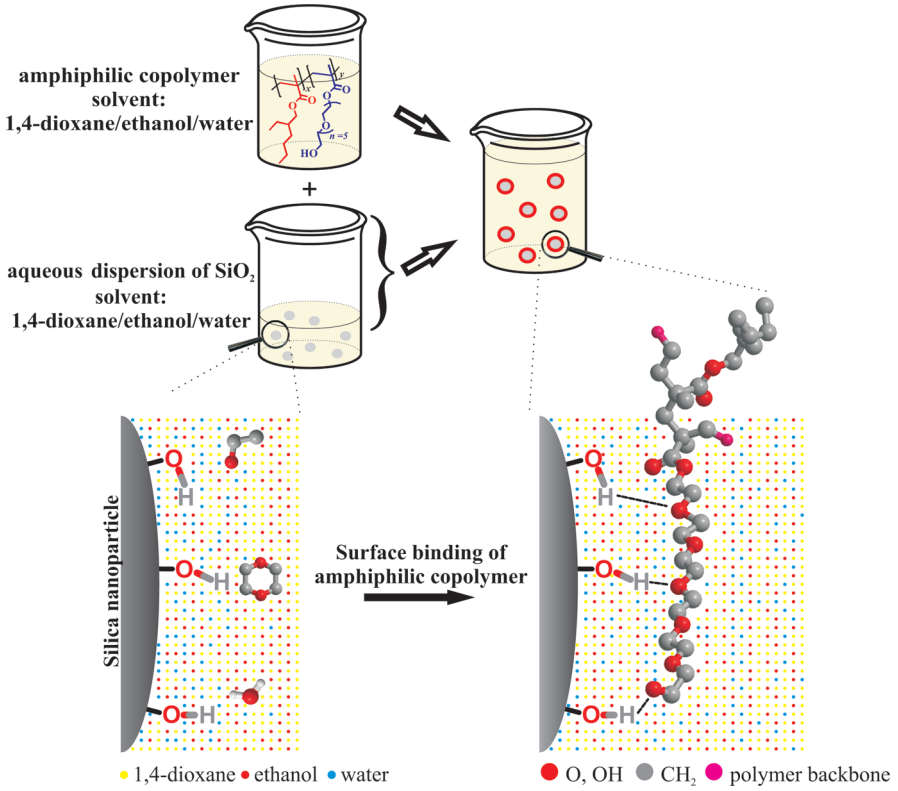

Figure 6. Schematic representation of the role of the monomers in the copolymer PEHMA-*co*-PPEOMA$^{n\approx5}$. EHMA imparted hydrophobicity to the SiO_2 particles; PEOMA, as the hydrophilic part, provided the interaction of the polymer with the SiO_2 surface.

obvious influence on the adsorption process. A screening of potential monomers for their ability to adsorb on the inorganic material is possible, without the need to synthesize the amphiphilic copolymer. In addition, the results clearly indicated that the adsorption strength of the amphiphilic copolymer (PEHMA-*co*-PPEOMA) was higher than the corresponding low molecular hydrophilic compound PEOMA (Table 2). Therefore, particles that carry high molecular weight compounds should reveal a lower tendency toward desorption by application of an external force (e.g., by extrusion) as indicated by the value for K_B, which is 2 orders of magnitude higher compared to the low molecular weight compounds. Furthermore, high molecular weight compounds with multiple binding sites were predominant due to a significant positive entropic contribution to the adsorption process, similar to multidentate ligands in chelate complexes. Aside from the *pure strength* of the interaction of potential anchor groups, the *accessibility* of these groups for the interaction with the particle surface was of great importance, as demonstrated for PPOMA vs PEOMA. The potential anchor groups were in both cases identical (oxygen of the EO groups and terminal OH group), but for PPOMA the EO groups were sterically shielded, making them inaccessible to form hydrogen bonding with the surface of the particles. This moderate steric hindrance already leads to a dramatic decrease of the adsorption strength. The comparison between the different classes of anchor groups, *nonionic vs zwitterionic vs acidic*, resulted in only a slight difference between the zwitterionic sulfate and acidic phosphate group. In the case of the nonionic PEOMA anchor group, the interaction with the SiO_2 particles insinuated a similar strength. It must be pointed out that, in contrast to 4VPSB and EGMP, PEOMA carried more than *one binding site* (five EO units and one terminal OH group). In case that only one binding site (HEMA) was present, the nonionic interaction was drastically weaker than the zwitterionic or acidic interaction. For a similar bonding strength HEMA has to be incorporated in much higher concentrations which, on the other hand, decrease the amount of hydrophobic monomer and, therefore, the interaction with a polymer matrix.

In summary, the described results open the possibility toward a more rational and optimized synthesis of nanocomposites. For example, the thermodynamic parameters should allow to estimate the number of anchor groups in a copolymer, which is essential for its irreversible and stable adsorption processes.

Conclusion

ITC was successfully introduced as a highly sensitive tool to study and characterize interactions in polymer and material science, as demonstrated for an organic−inorganic hybrid system. Herein, the adsorption of amphiphilic copolymers onto the surface of inorganic nanoparticles was investigated. In the case of the systems PEHMA-*co*-PPEOMA$^{n\approx5}$/SiO_2, PEHMA-*co*-4VPSB/SiO_2, and PEHMA-*co*-PEGMP/SiO_2, the enthalpy ΔH, the free energy ΔG, the entropy ΔS, and the binding constant K_B were successfully determined in a single experiment without the need to perform measurements at different temperatures. The obtained results gave rise to the quantification of the strength of the adsorption and to a detailed insight in the adsorption mechanism. Because of the fact that the design of nanocomposites is in many cases based on a noncovalent adsorption of surface-active compounds on the surface of an inorganic material, this knowledge might lead to a more rational and optimized design (concerning adsorption strength, amount of modification agent needed to fulfill a special purpose, surface coverage, irreversibility of the adsorption, etc.). For example, the ideal anchor group, concerning its nature, as well as an optimized ratio between the hydrophilic anchor group and the hydrophobic part in a desired copolymer might be identified. Furthermore, the

results pointed out that high molecular weight components with multiple binding sites are superior to low molecular weight compounds concerning adsorption. The K_B values for the high molecular weight compounds were 2 orders of magnitude higher than for the low molecular weight compounds, which indicated that the tendency to desorb is tremendously diminished in case of the high molecular weight compounds. Aside from the presented interaction between organic and inorganic compounds, ITC offers the potential to become also an important tool to analyze processes such as the aggregation behavior of polymers, which plays an important role in the formation of micelles and emulsions or in the self-assembly of amphiphilic block copolymers (e.g., polyelectrolytes).

References and Notes

(1) Bjelic, S.; Jelesarov, I. *J. Mol. Recognit*. **2008**, *21* (5), 289–311.
(2) Freire, E.; Mayorga, O. L.; Straume, M. *Anal. Chem*. **1990**, *62* (18), A950–A959.
(3) Wu, J. G.; Li, J. Y.; Li, G. Y.; Long, D. G.; Weis, R. M. *Biochemistry* **1996**, *35* (15), 4984–4993.
(4) Garciafuentes, L.; Reche, P.; Lopezmayorga, O.; Santi, D. V.; Gonzalezpacanowska, D.; Baron, C. *Eur. J. Biochem*. **1995**, *232* (2), 641–645.
(5) Qu, X. G.; Ren, J. S.; Riccelli, P. V.; Benight, A. S.; Chaires, J. B. *Biochemistry* **2003**, *42* (41), 11960–11967.
(6) Livingstone, J. R. *Nature* **1996**, *384* (6608), 491–492.
(7) Engman, K. C.; Sandin, P.; Osborne, S.; Brown, T.; Billeter, M.; Lincoln, P.; Norden, B.; Albinsson, B.; Wilhelmsson, L. M. *Nucleic Acids Res*. **2004**, *32* (17), 5087–5095.
(8) Ramstad, T.; Hadden, C. E.; Martin, G. E.; Speaker, S. M.; Teagarden, D. L.; Thamann, T. J. *Int. J. Pharm*. **2005**, *296* (1−2), 55–63.
(9) Muh, E.; Stieger, M.; Klee, J. E.; Frey, H.; Mulhaupt, R. *J. Polym. Sci., Part A: Polym. Chem*. **2001**, *39* (24), 4274–4282.
(10) Myszka, D. G. *Curr. Opin. Biotechnol*. **1997**, *8* (1), 50–57.
(11) Pauck, T.; Colfen, H. *Anal. Chem*. **1998**, *70* (18), 3886–3891.
(12) Wiseman, T.; Williston, S.; Brandts, J. F.; Lin, L. N. *Anal. Biochem*. **1989**, *179* (1), 131–137.
(13) Phillips, R. L.; Kim, I. B.; Tolbert, L. M.; Bunz, U. H. F. *J. Am. Chem. Soc*. **2008**, *130* (22), 6952–6954.
(14) Green, D. B.; Lane, J.; Wing, R. M. *Appl. Spectrosc*. **1987**, *41* (5), 847–851.
(15) Wiesner, P.; Kayser, H. *J. Biochem. Mol. Toxicol*. **2000**, *14* (4), 221–230.
(16) de Jong, L. A. A.; Kramer, K.; Kroeze, M. P. H.; Bischoff, R.; Uges, D. R. A.; Franke, J. P. *J. Pharm. Biomed. Anal*. **2005**, *39* (5), 964–971.
(17) Ogoshi, T.; Chujo, Y. *Compos. Interfaces* **2005**, *11* (8−9), 539–566.
(18) Meyer, E. E.; Rosenberg, K. J.; Israelachvili, J. *Proc. Natl. Acad. Sci. U.S.A*. **2006**, *103* (43), 15739–15746.
(19) Hoffmann, F.; Cornelius, M.; Morell, J.; Froba, M. *Angew. Chem., Int. Ed*. **2006**, *45* (20), 3216–3251.
(20) Shah, R. K.; Paul, D. R. *Polymer* **2006**, *47* (11), 4075–4084.
(21) Corkill, J. M.; Goodman, J. F.; Tate, J. R. *Trans. Faraday Soc*. **1966**, *62* (520P), 979–986.
(22) Killmann, E.; Winter, K. *Angew. Makromol. Chem*. **1975**, *43* (Mar 14), 53−73.
(23) Morimoto, T.; Naono, H. *Bull. Chem. Soc. Jpn*. **1972**, *45* (3), 700–705.
(24) Moudgil, B. M.; Behl, S.; Kulkarni, N. S. *J. Colloid Interface Sci*. **1992**, *148* (2), 337–342.
(25) Rouquerol, J. *Pure Appl. Chem*. **1985**, *57* (1), 69–77.
(26) Trens, P.; Denoyel, R. *Langmuir* **1993**, *9* (2), 519–522.
(27) Stelzig, S. H.; Klapper, M.; Müllen, K. *Adv. Mater*. **2008**, *20* (5), 929–932.
(28) Ajayan, P. M. S.; L., S.; Braun, P. V. *Nanocomposite Science and Technology*; Wiley-VCH: Berlin, 2003.
(29) Soto, V. M. M.; Glain, J. C. *Polymer* **1984**, *25* (1), 121–128.
(30) Khrenov, V.; Klapper, M.; Koch, M.; Müllen, K. *Macromol. Chem. Phys*. **2005**, *206* (1), 95–101.
(31) Chellani, M. *Application Note* **1999**, *10*, 14–18.
(32) Mizoue, L. S.; Tellinghuisen, J. *Anal. Biochem*. **2004**, *326* (1), 125–127.
(33) Jelesarov, I.; Bosshard, H. R. *J. Mol. Recognit*. **1999**, *12* (1), 3–18.
(34) Indyk, L.; Fisher, H. F. *Methods Enzymol*. **1998**, *295*, 350–364.
(35) Haq, I.; Ladbury, J. E.; Chowdhry, B. Z.; Jenkins, T. C.; Chaires, J. B. *J. Mol. Biol*. **1997**, *271* (2), 244–257.
(36) Privalov, P. L.; Gill, S. J. *Pure Appl. Chem*. **1989**, *61* (6), 1097–1104.
(37) Silverstein, K. A. T.; Haymet, A. D. J.; Dill, K. A. *J. Am. Chem. Soc*. **1998**, *120* (13), 3166–3175.
(38) Frank, H. S.; Evans, M. W. *J. Chem. Phys*. **1945**, *13* (11), 507–532.
(39) Leavitt, S.; Freire, E. *Curr. Opin. Struct. Biol*. **2001**, *11* (5), 560–566.
(40) Nemethy, G.; Scheraga, H. A. *J. Chem. Phys*. **1962**, *36* (12), 3382–3400.
(41) Sun, D. Z.; Wang, S. B.; Wei, X. L.; Yin, B. L. *J. Chem. Thermodyn*. **2005**, *37* (5), 431–436.
(42) Zajac, J.; Trompette, J. L.; Partyka, S. *J. Therm. Anal*. **1994**, *41* (6), 1277–1286.
(43) Denoyel, R.; Rouquerol, J. *J. Colloid Interface Sci*. **1991**, *143* (2), 555–572.
(44) Hergeth, W. D.; Zimmermann, R.; Bloss, P.; Schmutzler, K.; Wartewig, S. *Colloids Surf*. **1991**, *56*, 177–187.
(45) Siffert, B.; Li, J. F. *Colloids Surf*. **1989**, *40* (3−4), 207–217.
(46) Holdgate, G. A.; Tunnicliffe, A.; Ward, W. H. J.; Weston, S. A.; Rosenbrock, G.; Barth, P. T.; Taylor, I. W. F.; Pauptit, R. A.; Timms, D. *Biochemistry* **1997**, *36* (32), 9663–9673.
(47) Vartapetian, R. S.; Khozina, E. V.; Karger, J.; Geschke, D.; Rittig, F.; Feldstein, M. M.; Chalykh, A. E. *Macromol. Chem. Phys*. **2001**, *202* (12), 2648–2656.